Journal of Computational and Applied Mathematics 275 (2015) 321–334

Contents lists available at ScienceDirect

Journal of Computational and Applied Mathematics

journal homepage: www.elsevier.com/locate/cam

Spectral methods using Legendre wavelets for nonlinear Klein\Sine-Gordon equations

Fukang Yin *, Tian Tian, Junqiang Song, Min Zhu

Department of Software, College of Computer, National University of Defense Technology, Changsha, Hunan 410073, China

ARTICLE INFO

Article history:
Received 9 July 2014

Keywords:
Legendre wavelets
Spectral method
Hierarchical scale structure
Klein\Sine-Gordon equation

ABSTRACT

Klein/Sine-Gordon equations are very important in that they can accurately model many essential physical phenomena. In this paper, we propose a new spectral method using Legendre wavelets as basis for numerical solution of Klein\Sine-Gordon Equations. Due to the good properties of wavelets basis, the proposed method can obtain good spatial and spectral resolution. Moreover, the presented method can save more memory and computation time benefit from save more computation time benefit from the hierarchical scale structure of Legendre wavelets. 1D and 2D examples are included to demonstrate the validity and applicability of the new technique. Numerical results show the exponential convergence property and error characteristics of presented method.

1. Introduction

The Klein–Gordon equations can accurately model many essential phenomena in physical and chemical sciences. In this paper, we concentrate on the nonlinear Klein–Gordon equation as follows:

$$u_{tt} - \alpha u_{xx} - \beta u_{yy} + g\left(u\right) = f\left(x, y, t\right), \quad (x, y) \in \Omega,\ t \geq 0, \tag{1.1}$$

where u is a function of x, y and t, g is a nonlinear function and f is a known analytic function. The type of Eq. (1.1) depends on the forms of $g(u)$. In the case of $g\left(u\right) = \sin u$, Eq. (1.1) is the Sine-Gordon equation involving the d'Alembert operator. The Sine-Gordon equations have been successfully applied to model many physical problems [1–3], including applications in relativistic field theory, Josephson junctions or mechanical transmission lines [4]. It is known to all that soliton solutions appear in the 1D and 2D Sine-Gordon equations [5]. A wide range of analytical/numerical methods [6–22] have been proposed for the numerical solution of Klein–Gordon equations. Among these methods, the spectral methods [7,8], radial basis functions methods [15,17] and wavelets methods [23,24] deserved a lot of attention in the literature.

Due to the advantages of wavelets, such as orthogonality, multiresolution analysis and computational efficiency, it has made a lot of successes in many different fields of science and engineering [25–32]. Wavelets permit the accurate representation of a variety of functions and operators. Moreover, it can establish a connection with fast numerical algorithms [32]. The spectral method has the advantage of "exponential-convergence" property when smooth solutions are involved. Therefore, it has been playing an important role in the numerical solution of partial differential equations. The choice of the basis function is vitally important for spectral method. Orthogonal polynomials are usually chosen to be basis functions. The wavelet basis can combine the advantages of both infinitely differentiable and small compact support [33] which inherit

* Corresponding author. Tel.: +86 15084976786; fax: +86 0773 8745623.
E-mail addresses: yinfukang@nudt.edu.cn, yinfukang08@sina.com (F. Yin), cecejiasmin@163.com (T. Tian), junqiang@nudt.edu.cn (J. Song), zm@nudt.edu.cn (M. Zhu).

http://dx.doi.org/10.1016/j.cam.2014.07.014
0377-0427/

from both spectral and finite element basis. Further, the differentiation matrices of the spectral collocation method are dense in all dimensions, and it is generally complex and difficult to solve multi-dimensional problems by the Galerkin method. In contrast to aforementioned methods, Legendre wavelets method is easy to extend to multi-dimensional problems and its operational matrices are sparse, have lower dimension and equal on every subinterval [34]. Therefore, spectral collocation methods based on Legendre wavelet basis can obtain good spatial and spectral resolution while still keeping high efficiency.

Recently, A. Karimi Dizicheh et al. [35] proposed an iterative spectral collocation method based on Legendre Wavelets for solving IVP on large intervals. Motivated and inspired by the ongoing research in these areas, we develop a new effective and exponential convergent method, which combines the spectral method with the Legendre wavelets method, for numerical solution of Klein/Sine-Gordon equations. The organization of the remainder of this paper is as follows: In Section 2 we describe the basic formulation of Legendre wavelets and the operational matrices required for our subsequent development. The Legendre wavelets spectral collocation method is described in Section 3. Some numerical results of the proposed method for three 1-D examples and one 2-D example are given in Section 4. Conclusions and summary are made in Section 5.

2. Basis function of spectral method for limited domains

2.1. One-dimensional Legendre wavelets

In this section, the definition and some properties of 1D Legendre wavelets, which are first given by Razzaghi, M., and Yousefi, S., [32] are introduced here. For more details see Refs. [30,32].

2.1.1. The definition of one-dimensional Legendre wavelets

Legendre wavelets are derived from the shifted Legendre polynomials by dilation and translation, and have four arguments $\hat{n} = 2n - 1$, k can assume any positive integer, m is the order for Legendre polynomials and t is the normalized time. They are defined on the interval [0, 1) as follows:

$$\psi_{nm}(t) = \begin{cases} \sqrt{m + 1/2}\, 2^{\frac{k}{2}} L_m\left(2^k t - \hat{n}\right), & \text{for } \dfrac{\hat{n}-1}{2^k} \le t \le \dfrac{\hat{n}+1}{2^k}, \\ 0, & \text{otherwise} \end{cases} \tag{2.1}$$

where $m = 0, 1, 2, \ldots, M-1$, $n = 1, 2, \ldots, 2^{k-1}$. The coefficient $\sqrt{m + 1/2}$ is for orthonormality, the dilation parameter $a = 2^{-k}$ and the translation parameter $b = \hat{n}2^{-k}$. Here, $L_m(t)$ are the well-known Legendre polynomials of order m.

A function $f(t)$ defined over [0, 1) may be expanded by Legendre wavelet series as

$$f(t) = \sum_{n=1}^{+\infty} \sum_{m=0}^{+\infty} c_{nm} \psi_{nm}(t), \tag{2.2}$$

where

$$c_{nm} = \langle f(t), \psi_{nm}(t) \rangle, \tag{2.3}$$

in Eq. (2.3), $\langle \cdot, \cdot \rangle$ denotes the inner product.

If the infinite series in Eq. (2.2) is truncated, then it can be rewritten as

$$f(t) = \sum_{n=1}^{2^{k-1}} \sum_{m=0}^{M-1} c_{nm} \psi_{nm}(t) = \mathbf{C}^T \mathbf{\Psi}(t), \tag{2.4}$$

where $\mathbf{C}$ and $\mathbf{\Psi}(t)$ are $2^{k-1}M \times 1$ matrices defined as

$$\mathbf{C} = \left[c_{10}, c_{11}, \ldots, c_{1M-1}, c_{20}, \ldots, c_{2M-1}, \ldots, c_{2^{k-1}0}, \ldots, c_{2^{k-1}M-1}\right]^T \tag{2.5}$$

and

$$\mathbf{\Psi}(t) = \left[\psi_{10}(t), \psi_{11}(t), \ldots, \psi_{1M-1}(t), \ldots, \psi_{2^{k-1}0}(t), \ldots, \psi_{2^{k-1}M-1}(t)\right]^T. \tag{2.6}$$

2.1.2. Operational matrix of derivative

One dimensional Legendre wavelets operational matrix of derivative was derived by F. Mohammadi [30]. In this section, we just list the theorem and corollary as follows.

Theorem 1. *Let $\mathbf{\Psi}(t)$ be the Legendre wavelets vector defined in (2.6), then we have*

$$\frac{d\mathbf{\Psi}(t)}{dt} = \mathbf{D}\mathbf{\Psi}(t), \tag{2.7}$$

where $\mathbf{D}$ is $2^k(M+1)$ operational matrix of derivative defined as follows:

$$\mathbf{D} = \begin{bmatrix} \mathbf{F} & \mathbf{O} & \cdots & \mathbf{O} \\ \mathbf{O} & \mathbf{F} & \cdots & \mathbf{O} \\ \vdots & \vdots & \ddots & \vdots \\ \mathbf{O} & \mathbf{O} & \cdots & \mathbf{F} \end{bmatrix}, \tag{2.8}$$

in which $\mathbf{O}$ is an $(M+1)(M+1)$ zeros matrix, $\mathbf{F}$ is an $(M+1)(M+1)$ matrix and its (r,s)th element is defined as follows:

$$\mathbf{F}_{r,s} = \begin{cases} 2^{k+1}\sqrt{(2r-1)(2s-1)} & r = 2, \ldots, (M+1), s = 1, \ldots, r-1 \text{ and } (r+s) \text{ odd} \\ 0 & \text{otherwise.} \end{cases}$$

Corollary. *By using Eq. (2.7) the operational matrix for nth derivative can be derived as*

$$\frac{d^n\mathbf{\Psi}(t)}{dt^n} = \mathbf{D}^n\mathbf{\Psi}(t), \tag{2.9}$$

where $\mathbf{D}^n$ is the nth power of matrix $\mathbf{D}$.

2.2. Two-dimensional Legendre wavelets

In this section, we give the definition and list some theorems of 2D Legendre wavelets which are first introduced by Nanshan Liu [34]. See Refs. [24,34] for more details.

2.2.1. The definition of two-dimensional Legendre wavelets

Two-dimensional Legendre wavelets in $L^2(R)$ over the $[0, 1] \times [0, 1]$ in terms of one-dimensional Legendre wavelets can be expressed as [34]:

$$\Psi_{n,m,n',m'}(x, y) = \begin{cases} \Psi_{nm}(x)\Psi_{n'm'}(y), & \frac{n-1}{2^{k-1}} \le x \le \frac{n}{2^{k-1}}, \frac{n'-1}{2^{k'-1}} \le y \le \frac{n'}{2^{k'-1}}; \\ 0, & \text{otherwise,} \end{cases} \tag{2.10}$$

where $n = 1, 2, \ldots, 2^{k-1}$, $n' = 1, 2, \ldots, 2^{k'-1}$, $m = 0, 1, \ldots, M-1$ and $m' = 0, 1, \ldots, M'-1$.

The function $u(x, y) \in L^2(R)$ defined over $[0, 1] \times [0, 1]$ may be expanded as

$$u(x, y) = X(x)Y(y) \cong \sum_{n=1}^{\infty}\sum_{m=0}^{\infty}\sum_{n'=1}^{\infty}\sum_{m'=0}^{\infty} c_{n,m,n',m'}\Psi_{n,m,n'm'}(x, y). \tag{2.11}$$

If the infinite series in (2.11) is truncated, then it can be rewritten as

$$u(x, y) = X(x)Y(y) \cong \sum_{n=1}^{2^{k-1}}\sum_{m=0}^{M-1}\sum_{n'=1}^{2^{k'-1}}\sum_{m'=0}^{M'-1} c_{n,m,n',m'}\Psi_{n,m,n',m'}(x, y), \tag{2.12}$$

where $c_{n,m,n',m'} = \int_0^1\int_0^1 X(x)Y(y)\Psi_{n,m,n',m'}(x, y)dxdy$.

The truncated version of Eq. (2.12) can be expressed as the vector–matrix form

$$u(x, y) = \mathbf{C}^T\mathbf{\Psi}(x, y), \tag{2.13}$$

where $\mathbf{C}$ and $\mathbf{\Psi}(x, y)$ (see to [34] for more details) are coefficients matrix and wavelets vector–matrix respectively. The number of dimensions of $\mathbf{C}$ and $\mathbf{\Psi}(x, y)$ are $2^{k-1}2^{k'-1}MM' \times 1$, and given by

$$\begin{aligned} \mathbf{C} = [&c_{1,0,1,0}, \ldots, c_{1,0,1,M'-1}, c_{1,0,2,0}, \ldots, c_{1,0,2,M'-1}, \ldots, c_{1,0,2^{k'}-1,0}, \ldots, c_{1,0,2^{k'}-1,M'-1}, \ldots, \\ &c_{1,M-1,1,0}, \ldots, c_{1,M-1,1,M'-1}, c_{1,M-1,2,0}, \ldots, c_{1,M-1,2,M'-1}, \ldots, c_{1,M-1,2^{k'}-1,0}, \ldots, c_{1,M-1,2^{k'}-1,M'-1}, \ldots, \\ &c_{2,0,1,0}, \ldots, c_{2,0,1,M'-1}, c_{2,0,2,0}, \ldots, c_{2,0,2,M'-1}, \ldots, c_{2,0,2^{k'}-1,0}, \ldots, c_{2,0,2^{k'}-1,M'-1}, \ldots, \\ &c_{2,M-1,1,0}, \ldots, c_{2,M-1,1,M'-1}, c_{2,M-1,2,0}, \ldots, c_{2,M-1,2,M'-1}, \ldots, c_{2,M-1,2^{k'}-1,0}, \ldots, c_{2,M-1,2^{k'}-1,M'-1}, \ldots, \\ &c_{2^{k-1},0,1,0}, \ldots, c_{2^{k-1},0,1,M'-1}, c_{2^{k-1},0,2,0}, \ldots, c_{2^{k-1},0,2,M'-1}, \ldots, c_{2^{k-1},0,2^{k'-1},0}, \ldots, c_{2^{k-1},M-1,2^{k'-1},M'-1}]^T \end{aligned} \tag{2.14}$$

and

$$\begin{aligned}\boldsymbol{\Psi} = [&\Psi_{1,0,1,0}, \dots, \Psi_{1,0,1,M'-1}, \Psi_{1,0,2,0}, \dots, \Psi_{1,0,2,M'-1}, \dots, \Psi_{1,0,2^{k'-1},0}, \dots, \Psi_{1,0,2^{k'-1},M'-1}, \dots,\\ &\Psi_{1,M-1,1,0}, \dots, \Psi_{1,M-1,1,M'-1}, \Psi_{1,M-1,2,0}, \dots, \Psi_{1,M-1,2,M'-1}, \dots, \Psi_{1,M-1,2^{k'-1},0}, \dots, \Psi_{1,M-1,2^{k'-1},M'-1}, \dots,\\ &\Psi_{2,0,1,0}, \dots, \Psi_{2,0,1,M'-1}, c_{2,0,2,0}, \dots, \Psi_{2,0,2,M'-1}, \dots, \Psi_{2,0,2^{k'-1},0}, \dots, \Psi_{2,0,2^{k'-1},M'-1}, \dots,\\ &\Psi_{2,M-1,1,0}, \dots, \Psi_{2,M-1,1,M'-1}, \Psi_{2,M-1,2,0}, \dots, \Psi_{2,M-1,2,M'-1}, \dots, \Psi_{2,M-1,2^{k'-1},0}, \dots, \Psi_{2,M-1,2^{k'-1},M'-1}, \dots,\\ &\Psi_{2^{k-1},0,1,0}, \dots, \Psi_{2^{k-1},0,1,M'-1}, \Psi_{2^{k-1},0,2,0}, \dots, \Psi_{2^{k-1},0,2,M'-1}, \dots, \Psi_{2^{k-1},0,2^{k'-1},0}, \dots, \Psi_{2^{k-1},M-1,2^{k'-1},M'-1}]^T.\end{aligned} \tag{2.15}$$

2.2.2. Operational matrices of derivative

Two-dimensional Legendre wavelets operational matrices of derivative were derived by Yin [24]. In this section, we just list the theorems and corollary as follows.

Theorem 2. *Let $\boldsymbol{\Psi}(x, y)$ be the two-dimensional Legendre wavelets vector defined in Eq. (2.15), we have*

$$\frac{\partial \boldsymbol{\Psi}(x, y)}{\partial x} = \mathbf{D}_x \boldsymbol{\Psi}(x, y), \tag{2.16}$$

where $\mathbf{D}_x$ is $2^{k-1}2^{k'-1}MM' \times 2^{k-1}2^{k'-1}MM'$ and has the form as follows:

$$\mathbf{D}_x = \begin{bmatrix} \mathbf{D} & \mathbf{O}' & \cdots & \mathbf{O}' \\ \mathbf{O}' & \mathbf{D} & \cdots & \mathbf{O}' \\ \vdots & \vdots & \ddots & \vdots \\ \mathbf{O}' & \mathbf{O}' & \cdots & \mathbf{D} \end{bmatrix}$$

in which $\mathbf{O}'$ and $\mathbf{D}$ is a $2^{k'-1}MM' \times 2^{k'-1}MM'$ matrix and the element of $\mathbf{D}$ is defined as follows:

$$\mathbf{D}_{r,s} = \begin{cases} 2^k\sqrt{(2r-1)(2s-1)}\,\mathbf{I}, & r = 2, 3, \dots, M;\ s = 1, \dots, r-1,\ r+s \text{ is odd} \\ \mathbf{O}, & \text{otherwise} \end{cases}$$

and $\mathbf{I}$, $\mathbf{O}$ is a $2^{k'-1}M' \times 2^{k'-1}M'$ identity matrix.

Theorem 3. *Let $\boldsymbol{\Psi}(x, y)$ be the two-dimensional Legendre wavelets vector defined in Eq. (2.15), we have*

$$\frac{\partial \boldsymbol{\Psi}(x, y)}{\partial y} = \mathbf{D}_y \boldsymbol{\Psi}(x, y), \tag{2.17}$$

in which

$$\mathbf{D}_y = \begin{bmatrix} \mathbf{D} & \mathbf{O}' & \cdots & \mathbf{O}' \\ \mathbf{O}' & \mathbf{D} & \cdots & \mathbf{O}' \\ \vdots & \vdots & \ddots & \vdots \\ \mathbf{O}' & \mathbf{O}' & \cdots & \mathbf{D} \end{bmatrix},$$

where $\mathbf{D}_y$ is $2^{k-1}2^{k'-1}MM' \times 2^{k-1}2^{k'-1}MM'$ and $\mathbf{O}'$, $\mathbf{D}$ is an $MM' \times MM'$ matrix and is given as

$$\mathbf{D} = \begin{bmatrix} \mathbf{F} & \mathbf{O} & \cdots & \mathbf{O} \\ \mathbf{O} & \mathbf{F} & \cdots & \mathbf{O} \\ \vdots & \vdots & \ddots & \vdots \\ \mathbf{O} & \mathbf{O} & \cdots & \mathbf{F} \end{bmatrix}$$

in which $\mathbf{O}$ and $\mathbf{F}$ is an $M' \times M'$ matrix, and $\mathbf{F}$ is defined as follows:

$$\mathbf{F}_{r,s} = \begin{cases} 2^{k'}\sqrt{(2r-1)(2s-1)}, & r = 2, \dots, M';\ S = 1, \dots, r-1;\ \text{and } r+s \text{ is odd} \\ 0, & \text{otherwise.} \end{cases}$$

Corollary 1. *By using Eqs. (2.16) and (2.17) the operational matrices for nth derivative can be derived as*

$$\frac{\partial^n \boldsymbol{\Psi}(x, y)}{\partial x^n} = \mathbf{D}_x^n \boldsymbol{\Psi}(x, y), \qquad \frac{\partial^m \boldsymbol{\Psi}(x, y)}{\partial y^m} = \mathbf{D}_y^m \boldsymbol{\Psi}(x, y) \tag{2.18}$$

$$\frac{\partial^{n+m} \boldsymbol{\Psi}(x, y)}{\partial x^n \partial y^m} = \mathbf{D}_x^n \mathbf{D}_y^m \Psi(x, y) \tag{2.19}$$

where $\mathbf{D}^n$ is the nth power of matrix $\mathbf{D}$.

3. Legendre wavelets spectral collocation method (LWSCM)

Mehrdad Lakestani [19] presented effective and accurate numerical techniques based on the finite difference by employing cubic B-spline scaling functions for the solution of nonlinear Klein–Gordon equation. Motivated and inspired by their work, we propose a new effective and exponential convergent method, which combines the spectral method with the Legendre wavelets method, for numerical solution of Klein\Sine-Gordon equations. Compared with the cubic B-spline scaling functions, the operational matrices of the Legendre wavelets are sparse, equal on every subinterval, and most importantly, easy to compute. What is more, the hierarchical scale structure of Legendre wavelets can be exploited to develop a fast algorithm.

3.1. One-dimensional LWSCM

Consider the following form of equation:

$$u_{tt} - \alpha u_{xx} + g\left(u\right) = f\left(x, t\right), \quad x \in \Omega = \left[x_L, x_R\right],\ t \geq 0. \tag{3.1}$$

The initial condition is

$$\begin{aligned} &u\left(x, 0\right) = g_1\left(x\right), \quad x \in \Omega,\ t > 0 \\ &\frac{\partial u\left(x, 0\right)}{\partial t} = g_2\left(x\right), \quad x \in \Omega,\ t > 0, \end{aligned} \tag{3.2}$$

and boundary condition is

$$u\left(x, t\right) = h\left(x, t\right), \quad x \in \partial\Omega,\ t > 0. \tag{3.3}$$

In order to use Legendre wavelets basis defined for $X \in [0, 1]$. Hence on the arbitrary interval $x \in \Omega = [x_L, x_R]$, one can use the transform

$$x : [x_L, x_R] \to [0, 1], \qquad X\left(x\right) = \frac{x - x_L}{x_R - x_L}.$$

By employing θ-weighted scheme, Eq. (3.1) can be discretized as

$$\frac{u^{n+1} - 2u^n + u^{n-1}}{(\Delta t)^2} - \theta\left(\alpha\frac{\partial^2 u^{n+1}}{\partial x^2}\right) - (1-\theta)\left(\alpha\frac{\partial^2 u^n}{\partial x^2}\right) + g\left(u^n\right) = f^n, \tag{3.4}$$

where $0 \leq \theta \leq 1$, Δt is the time step size and note that $u^n\left(x\right) = u\left(t_n, x\right),\ t_n = n \times \Delta t$.

Eq. (3.4) can be rewritten as

$$u^{n+1} - \theta\left(\Delta t\right)^2\left(\alpha\frac{\partial^2 u^{n+1}}{\partial x^2}\right) = 2u^n + (1-\theta)\left(\Delta t\right)^2\left(\alpha\frac{\partial^2 u^n}{\partial x^2}\right) - (\Delta t)^2 g\left(u^n\right) + (\Delta t)^2 f^n - u^{n-1}. \tag{3.5}$$

According to Eq. (2.4), the term u^n can be expanded by Legendre wavelets as

$$u^n(x) = \mathbf{C}_n^T\mathbf{\Psi}(x). \tag{3.6}$$

By substituting Eq. (3.6) into Eq. (3.5), one can have

$$\mathbf{C}_{n+1}^T\mathbf{H}_L\Psi\left(x\right) = \left(C_n^T\mathbf{H}_R - \mathbf{C}_{n-1}^T\right)\Psi\left(x\right) - (\Delta t)^2 g\left(\mathbf{C}_n^T\Psi\left(x\right)\right) + (\Delta t)^2 f^n \tag{3.7}$$

in which $\mathbf{H}_L = I - \alpha\theta\left(\Delta t\right)^2\mathbf{D}^2$ and $\mathbf{H}_R = 2I + \alpha\left(1-\theta\right)\left(\Delta t\right)^2\mathbf{D}^2$, where $\mathbf{D}$ is the derivative matrix defined in Eq. (2.7).

Using the boundary condition (3.3), one can get

$$\mathbf{C}_{n+1}^T\mathbf{\Psi}\left(0\right) = h\left(0, t_{n+1}\right), \qquad \mathbf{C}_{n+1}^T\mathbf{\Psi}\left(1\right) = h\left(1, t_{n+1}\right), \tag{3.8}$$

Collocating Eq. (3.7) in $2^{k-1}M - 2$ Gauss–Legendre points $\{x_i\}_{i=2}^{2^{k-1}M-1}$, one can obtain

$$\mathbf{C}_{n+1}^T\mathbf{H}_L\Psi\left(x_i\right) = \left(\mathbf{C}_n^T\mathbf{H}_R - \mathbf{C}_{n-1}^T\right)\Psi\left(x_i\right) - (\Delta t)^2 g\left(\mathbf{C}_n^T\mathbf{\Psi}\left(x_i\right)\right) + (\Delta t)^2 f^n\left(x_i, t_n\right). \tag{3.9}$$

Eqs. (3.8) and (3.9) can be written as matrix form

$$\mathbf{A}\mathbf{C}_{n+1} = \mathbf{B}, \tag{3.10}$$

where $\mathbf{A}$ and $\mathbf{B}$ are $2^{k-1}M \times 2^{k-1}M$ and $2^{k-1}M \times 1$ matrices, respectively.

Using the first initial condition of Eq. (3.2), we have

$$\mathbf{C}_0^T \mathbf{\Psi}(x) = g_1(x). \tag{3.11}$$

By using the second initial condition of Eq. (3.2), one can get

$$\frac{u^1 - u^{-1}}{2\Delta t} = g_2(x), \quad x \in \Omega. \tag{3.12}$$

Eq. (3.12) can be rewritten as

$$\mathbf{C}_{-1}^T \mathbf{\Psi}(x) = \mathbf{C}_1^T \mathbf{\Psi}(x) - 2\Delta t g_2(x). \tag{3.13}$$

Eq. (3.10) using Eq. (3.11) gives a linear system of equations with $2^{k-1}M$ unknowns and equations, which can be solved to find $\mathbf{C}_{n+1}$ in each step $n = 0, 1, 2, \ldots$, so the unknown functions $u(x, t_n)$ in any time $t = t_n$ can be found.

3.2. Two-dimensional LWSCM

Consider the following form of equation:

$$u_{tt} - \alpha u_{xx} - \beta u_{yy} + g(u) = f(x, y, t), \quad (x, y) \in \Omega,\ t \geq 0. \tag{3.14}$$

The initial condition is

$$u(x, y, 0) = g_1(x, y), \quad x \in \Omega,\ t > 0, \tag{3.15}$$

$$\frac{\partial u(x, y, 0)}{\partial t} = g_2(x, y), \quad x \in \Omega,\ t > 0, \tag{3.16}$$

and boundary condition is

$$u(x, y, t) = h(x, y, t), \quad (x, y) \in \partial\Omega,\ t > 0. \tag{3.17}$$

In order to use Legendre wavelets basis defined for $(X, Y) \in [0, 1] \times [0, 1]$. Hence on the arbitrary interval $(x, y) \in \Omega = [x_L, x_R] \times [y_L, y_R]$, one can use the transform

$$(X, Y) : [x_L, x_R] \times [y_L, y_R] \to [0, 1] \times [0, 1], \qquad X(x) = \frac{x - x_L}{x_R - x_L}, \qquad Y(x) = \frac{y - y_L}{y_R - y_L}.$$

By employing θ-weighted scheme, Eq. (3.14) can be discretized as

$$\frac{u^{n+1} - 2u^n + u^{n-1}}{(\Delta t)^2} - \theta\left(\alpha\frac{\partial^2 u^{n+1}}{\partial x^2} + \beta\frac{\partial^2 u^{n+1}}{\partial y^2}\right) - (1-\theta)\left(\alpha\frac{\partial^2 u^n}{\partial x^2} + \beta\frac{\partial^2 u^n}{\partial y^2}\right) + g\left(u^n\right) = f^n \tag{3.18}$$

where $0 \leq \theta \leq 1$, Δt is the time step size and note $u^n(x, y) = u(t_n, x, y)$, $t_n = n \times \Delta t$. Eq. (3.18) can be rewritten as

$$u^{n+1} - \theta(\Delta t)^2\left(\alpha\frac{\partial^2 u^{n+1}}{\partial x^2} + \beta\frac{\partial^2 u^{n+1}}{\partial y^2}\right) = \begin{cases} 2u^n + (1-\theta)(\Delta t)^2\left(\alpha\frac{\partial^2 u^n}{\partial x^2} + \beta\frac{\partial^2 u^n}{\partial y^2}\right) \\ -(\Delta t)^2 g\left(u^n\right) + (\Delta t)^2 f^n - u^{n-1}. \end{cases} \tag{3.19}$$

According to Eq. (2.13), the term u^n can be expanded by Legendre wavelets as

$$u(x, y) \cong \mathbf{C}^T \mathbf{\Psi}(x, y). \tag{3.20}$$

By substituting Eq. (3.20) into Eq. (3.19), one can have

$$\mathbf{C}_{n+1}^T \mathbf{H}_L \mathbf{\Psi}(x, y) = \left(\mathbf{C}_n^T \mathbf{H}_R - \mathbf{C}_{n-1}^T\right)\mathbf{\Psi}(x, y) - (\Delta t)^2 g\left(\mathbf{C}_n^T \mathbf{\Psi}(x, y)\right) + (\Delta t)^2 f^n \tag{3.21}$$

with $\mathbf{H}_L = \mathbf{I} - \theta(\Delta t)^2\left(\alpha\mathbf{D}_x^2 + \beta\mathbf{D}_x^2\right)$ and $\mathbf{H}_R = 2\mathbf{I} + (1-\theta)(\Delta t)^2\left(\alpha\mathbf{D}_x^2 + \beta\mathbf{D}_x^2\right)$, in which $\mathbf{I}$ is an $N \times N'$ identity matrix, where $N = 2^{k-1}M$ and $N' = 2^{k'-1}M'$, where $\mathbf{D}_x^2 = (\mathbf{D}_x)^2$ and $\mathbf{D}_y = \left(\mathbf{D}_y\right)^2$, matrices $\mathbf{D}_x$ and $\mathbf{D}_y$ are two-dimensional derivative matrices with respect to x and y, respectively.

Using the boundary condition (3.17), one can get

$$\begin{aligned} &\mathbf{C}_{n+1}^T \mathbf{\Psi}\left(0, y_j\right) = h\left(0, y_j, t_{n+1}\right), \qquad \mathbf{C}_{n+1}^T \mathbf{\Psi}\left(1, y_j\right) = h\left(1, y_j, t_{n+1}\right), \quad j = 1, 2, \ldots, N', \\ &\mathbf{C}_{n+1}^T \mathbf{\Psi}(x_i, 0) = h(x_i, 0, t_{n+1}), \qquad \mathbf{C}_{n+1}^T \mathbf{\Psi}(x_i, 1) = h(x_i, 1, t_{n+1}), \quad i = 1, 2, \ldots, N. \end{aligned} \tag{3.22}$$

Collocating Eq. (3.21) in $(N-2) \times \left(N'-2\right)$ Gauss–Legendre points $\{x_i\}_{i=2}^{N-1} \times \left\{y_j\right\}_{j=2}^{N'-1}$, one can obtain

$$\mathbf{C}_{n+1}^T \mathbf{H}_L \Psi\left(x_i, y_j\right) = \left(\mathbf{C}_n^T \mathbf{H}_R - \mathbf{C}_{n-1}^T\right)\mathbf{\Psi}\left(x_i, y_j\right) - (\Delta t)^2 g\left(\mathbf{C}_n^T \mathbf{\Psi}\left(x_i, y_j\right)\right) + (\Delta t)^2 f^n\left(x_i, y_j, t_n\right). \tag{3.23}$$

Table 1
Errors of Example 1 for difference time with $\Delta t = 0.0001$.

t	L_∞-error		L_2-error		RMS		Time (s)	
	RBFs (100)	LWSCM (24)	RBFs (100)	LWSCM (24)	RBFs (100)	LWSCM (24)	RBFs (100)	LWSCM (24)
1	5.0705e−5	9.4526e−5	2.9474e−4	1.7947e−4	2.0789e−5	3.6633e−5	23	05.16
2	5.0260e−4	9.7933e−4	2.7082e−3	2.0683e−3	1.9102e−4	4.2219e−4	51	10.33
3	2.0612e−3	3.9740e−3	9.7246e−3	7.9118e−3	6.8592e−4	1.6150e−3	84	15.21
4	6.5720e−3	1.2960e−2	2.7881e−2	2.4427e−2	1.9666e−3	4.9861e−3	120	20.41
5	1.9067e−2	3.7224e−2	7.7337e−2	6.9930e−2	5.4549e−3	1.4274e−2	160	26.03

Eqs. (3.23) and (3.22) can be written as matrix form

$$\mathbf{A}\mathbf{C}_{n+1} = \mathbf{B}, \tag{3.24}$$

where $\mathbf{A}$ and $\mathbf{B}$ are $\left(N \times N'\right) \times \left(N \times N'\right)$ and $\left(N \times N'\right) \times 1$ matrices, respectively.

By employing the initial condition of Eq. (3.15), we have

$$\mathbf{C}_0^T \boldsymbol{\Psi}(x, y) = g_1(x, y). \tag{3.25}$$

By using the initial condition of Eq. (3.16), one can get

$$\frac{u^1 - u^{-1}}{2\Delta t} = g_2(x, y), \quad (x, y) \in \Omega. \tag{3.26}$$

Eq. (3.26) can be rewritten as

$$\mathbf{C}_{-1}^T \boldsymbol{\Psi}(x) = \mathbf{C}_1^T \boldsymbol{\Psi}(x) - 2\Delta t g_2(x). \tag{3.27}$$

Eq. (3.24) using Eq. (3.27) gives a linear system of equations with $N \times N'$ unknowns and equations, which can be solved to find $\mathbf{C}_{n+1}$ in each step $n = 0, 1, 2, \ldots$, so the unknown functions $u(x, y, t_n)$ in any time $t = t_n$ can be found.

4. Numerical examples

In this section, three 1-D examples and one 2-D example are discussed to validate the presented method. Error functions are defined as

$$e_j = (u_{exact})_j - \left(u_{approx}\right)_j, \quad e = u_{exact} - u_{approx},$$

$$\|e\|_{L_\infty} = \max_j \left|e_j\right|, \qquad \|e\|_{L_2} = \sqrt{\sum_{j=1}^{N} \left|\left(e_j\right)^2\right|}, \qquad \|e\|_{\mathrm{RMS}} = \sqrt{\frac{1}{N}\sum_{j=1}^{N} \left|\left(e_j\right)^2\right|}.$$

4.1. 1D cases

Example 1. Consider the following one-dimensional nonlinear Klein–Gordon equation [17]:

$$\frac{\partial^2 u}{\partial t^2} - \frac{\partial^2 u}{\partial x^2} + u + u^3 = f(x, t), \quad x \in \Omega = [-1, 1] \subset \mathrm{R}, \; 0 < t \le T, \tag{4.1}$$

where $f(x, t) = \left(x^2 - 2\right)\cosh(x + t) - 4x\sinh(x + t) + x^6\cosh^3(x + t)$, subject to the initial conditions

$$\begin{cases} u(x, 0) = x^2\cosh(x), & -1 \le x \le 1 \\ u_t(x, 0) = x^2\sinh(x), & -1 \le x \le 1, \end{cases} \tag{4.2}$$

and the Dirichlet boundary condition

$$u(x, t) = h(x, t), \quad x \in \partial\Omega, \; 0 < t \le T. \tag{4.3}$$

The exact solution of Eq. (4.1) is

$$u(x, t) = x^2\cosh(x + t). \tag{4.4}$$

Table 1 gives the errors at difference time by using RBFs method [17] and LWSCM. Fig. 1 presents the numerical solutions of Example 1 at time $t = 2, 3, 4$ and 5 with $N = 24$ and $\Delta t = 0.0001$. From Table 1, it can be found that L_2-error of LWSCM is smaller than RBFs while L_∞-error of LWSCM is bigger than RBFs. Although RMS error is only a little bigger than one obtained by RBFs, LWSCM needs much less number of grid points and time than RBF.

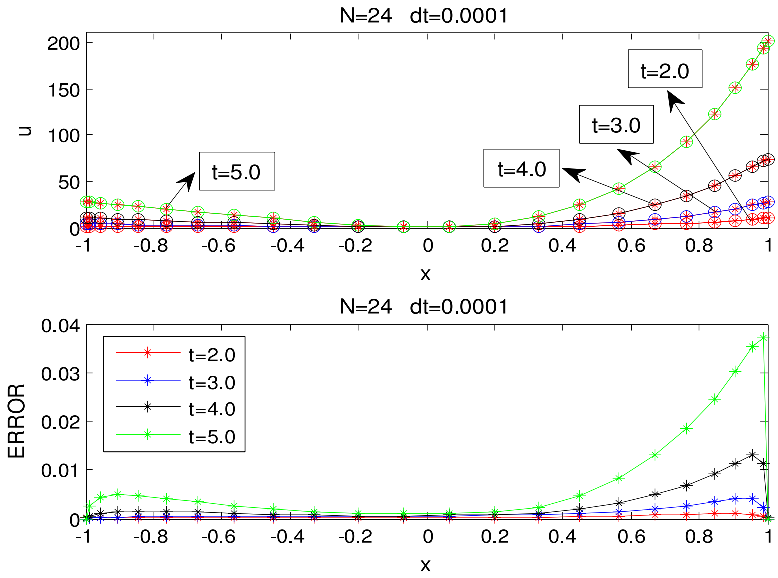

Fig. 1. Numerical solutions of Example 1 at different times with $\Delta t = 0.0001$, $N = 24$.

Table 2
Errors of Example 2 for $c = 0.5, 0.05$ at different times t with $\Delta t = 0.0001$.

t	L_∞-error		L_2-error		RMS	
	RBFs (50)	LWSCM (9)	RBFs (50)	LWSCM (9)	RBFs (50)	LWSCM (9)
$c = 0.5$						
1	5.9964e−06	6.1162e−06	4.0761e−05	1.0686e−05	4.0559e−06	3.5619e−06
2	2.1973e−05	2.2173e−05	1.5769e−04	4.0545e−05	1.5691e−05	1.3515e−05
3	9.0893e−05	9.1296e−05	6.4792e−04	1.6246e−04	6.4470e−05	5.4154e−05
4	8.2945e−04	7.7859e−04	5.3572e−03	1.3453e−03	5.3306e−04	4.4843e−04
$c = 0.05$						
1	3.6497e−07	1.0784e−07	1.7861e−06	1.6653e−07	1.7772e−07	5.5509e−08
2	3.8952e−07	1.9920e−07	1.5383e−06	3.5710e−07	1.5306e−07	1.1903e−07
3	4.2123e−07	2.3722e−07	1.7275e−06	4.1971e−07	1.7190e−07	1.3990e−07
4	4.5928e−07	1.9190e−07	2.0097e−06	3.2353e−07	1.9997e−07	1.0784e−07

Example 2. Consider the following one-dimensional nonlinear Klein–Gordon equation [17,19]

$$\frac{\partial^2 u}{\partial t^2} - 2.5\frac{\partial^2 u}{\partial x^2} + u + 1.5u^3 = 0, \quad x \in \Omega = [0, 1] \subset \mathrm{R},\ 0 < t \le T, \tag{4.5}$$

subject to the initial conditions

$$\begin{cases} u(x, 0) = \sqrt{\dfrac{\beta}{\gamma}} \tan\left(\sqrt{-\dfrac{\beta}{2(\alpha + c^2)}}x\right), & 0 \le x \le 1 \\ u_t(x, 0) = c\sqrt{\dfrac{\beta}{\gamma}}\sqrt{-\dfrac{\beta}{2(\alpha + c^2)}} \sec^2\left(\sqrt{-\dfrac{\beta}{2(\alpha + c^2)}}x\right), & 0 \le x \le 1, \end{cases} \tag{4.6}$$

and the Dirichlet boundary condition

$$u(x, t) = h(x, t), \quad x \in \partial\Omega,\ 0 < t \le T. \tag{4.7}$$

The exact solution of Eq. (4.5) is

$$u(x, t) = \sqrt{\frac{\beta}{\gamma}} \tan\left(\sqrt{-\frac{\beta}{2(\alpha + c^2)}}(x + ct)\right). \tag{4.8}$$

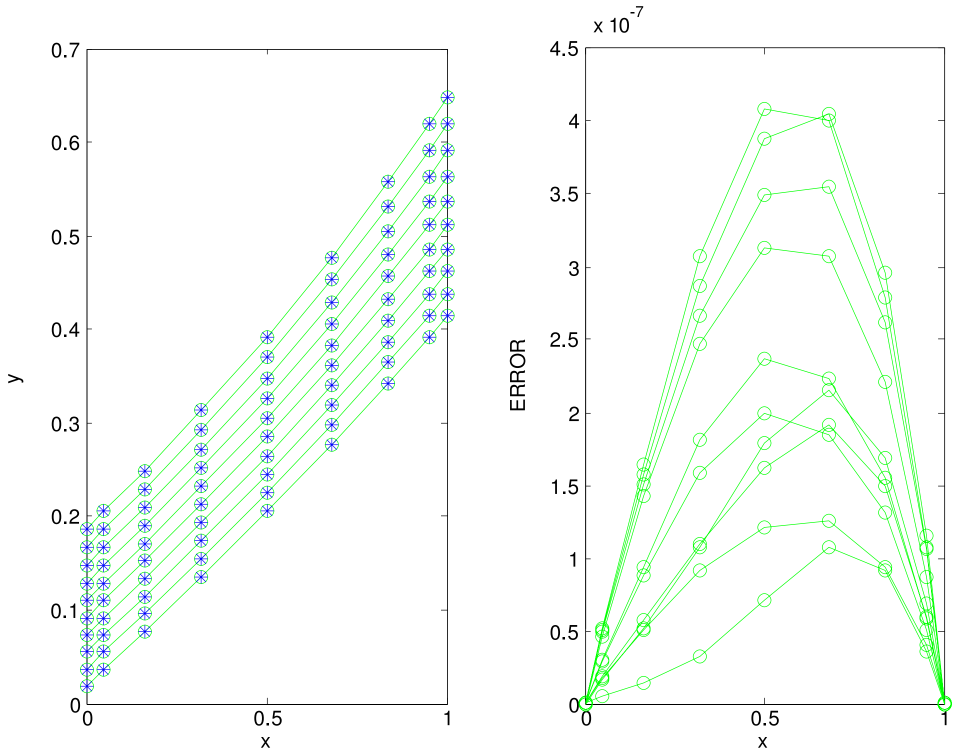

Fig. 2. Numerical solution of Example 2 with $c = 0.05$, $N = 24$ and $\Delta t = 0.0001$ for $t = 1$–10. From bottom to top are the numerical results at the time of 1–10, respectively.

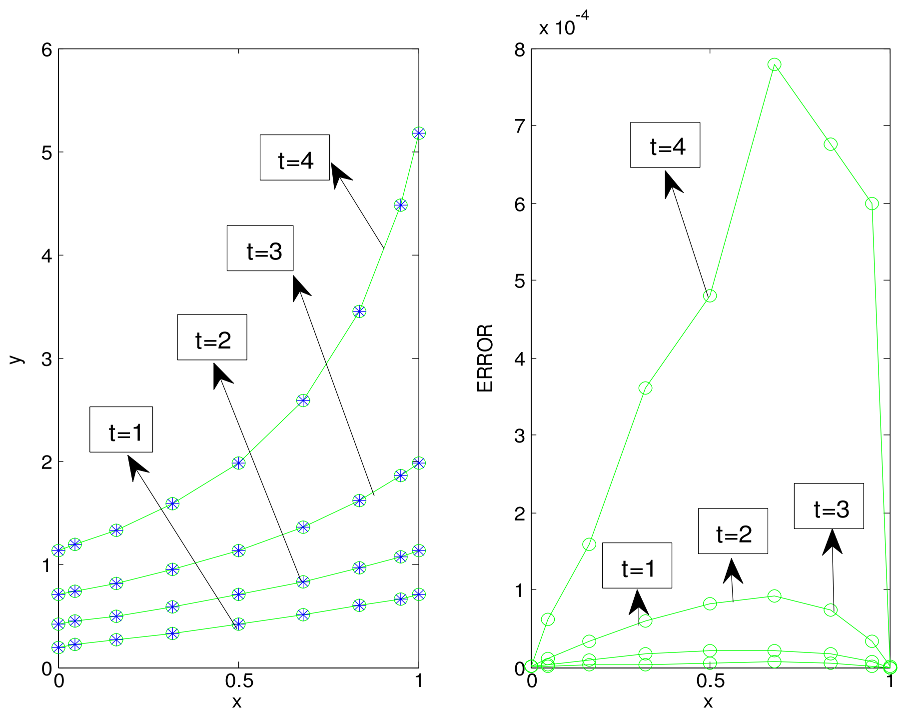

Fig. 3. Numerical solution of Example 2 with $c = 0.5$, $N = 24$ and $\Delta t = 0.0001$ for $t = 1$–4.

Fig. 2 shows the numerical solution from $t = 1$ to 10 by using LWSCM with $c = 0.05$, $N = 24$ and $\Delta t = 0.0001$. Fig. 3 depicts the numerical solution from $t = 1$ to 4 by using LWSCM with $c = 0.5$, $N = 24$ and $\Delta t = 0.0001$. Table 2 lists the

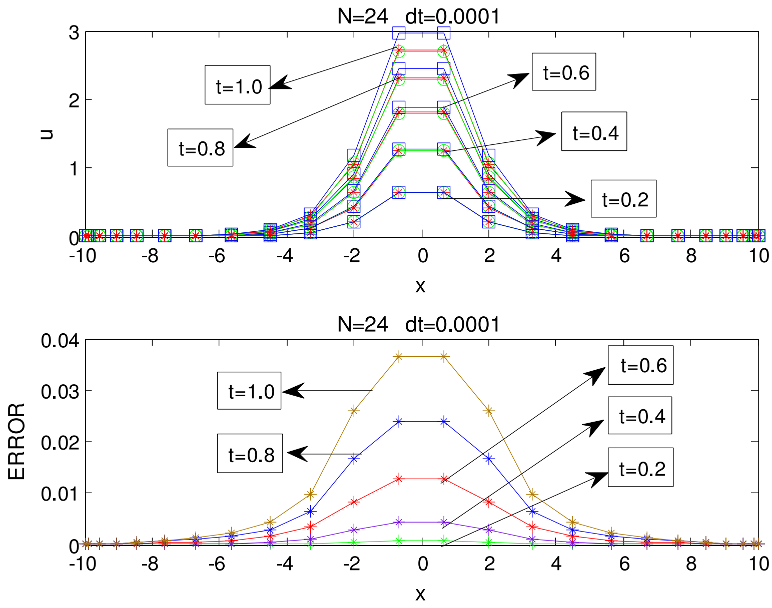

Fig. 4. Numerical solution of Example 3 for difference t.

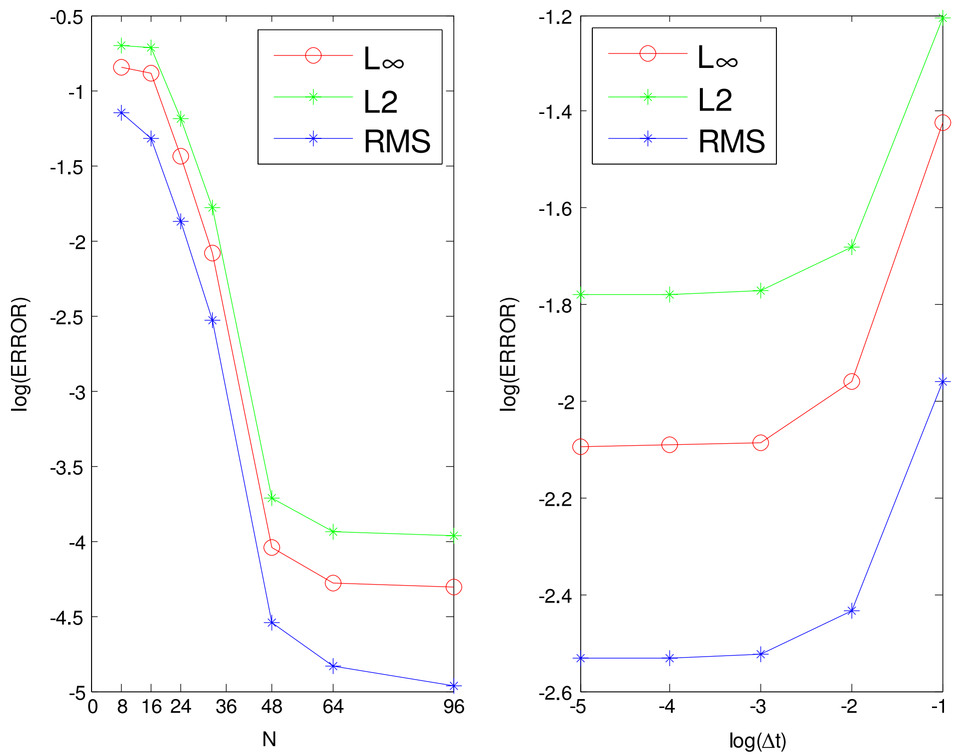

Fig. 5. Root-mean-square errors (in log form) of Example 3 as a function of N at $t = 1.0$ with $\Delta t = 0.0001$ and as a function of Δt at $t = 1.0$ with $N = 32$.

numerical solutions of Example 2 at $t = 1$–4 with $N = 24$ and $\Delta t = 0.0001$ for $c = 0.5$ and 0.05. From Table 2, it can be found that LWSCM is more accurate than RBFs [17] while only need much less grid points than RBFs.

Example 3. Consider the following one-dimensional nonlinear Sine-Gordon equation [11,13–15]:

$$\frac{\partial^2 u}{\partial t^2} - \frac{\partial^2 u}{\partial x^2} + \sin u = 0, \quad x \in \Omega = [-10, 10] \subset \mathrm{R}, 0 < t \leq T, \tag{4.9}$$

Table 3
L_∞, L_2 and RMS errors using the explicit method, the RBF method and LWSCM with $\Delta t = 0.001$.

t	Explicit method		RBF method ($N = 56 \times 56$)			LWSCM ($N = 24 \times 24$)			LWSCM ($N = 32 \times 32$)		
	L_2	L_∞	L_2	L_∞	RMS	L_2	L_∞	RMS	L_2	L_∞	RMS
1	0.7221	0.0350	0.2860	0.0670	0.0050	0.0178	0.0046	0.0007	0.0051	0.0008	0.0002
3	0.7877	0.0431	0.5872	0.0834	0.0103	0.0424	0.0090	0.0018	0.0153	0.0022	0.0005
5	0.5167	0.0404	0.8288	0.1015	0.0145	0.0598	0.0094	0.0025	0.0307	0.0048	0.0010
7	0.6531	0.0353	1.0706	0.1516	0.0187	0.0801	0.0121	0.0033	0.0504	0.0090	0.0016

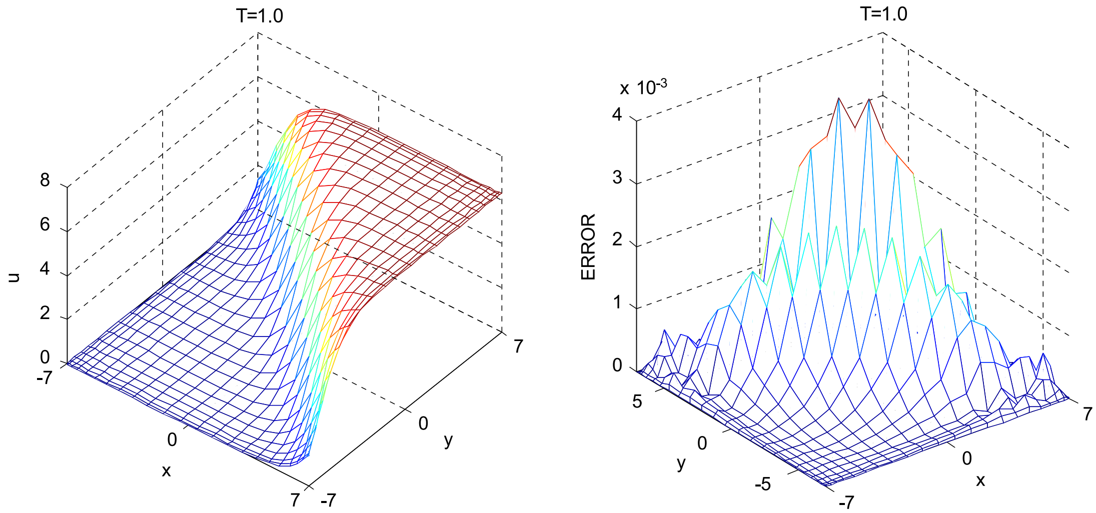

(a) Numerical results for LWSCM at time $t = 1.0$.

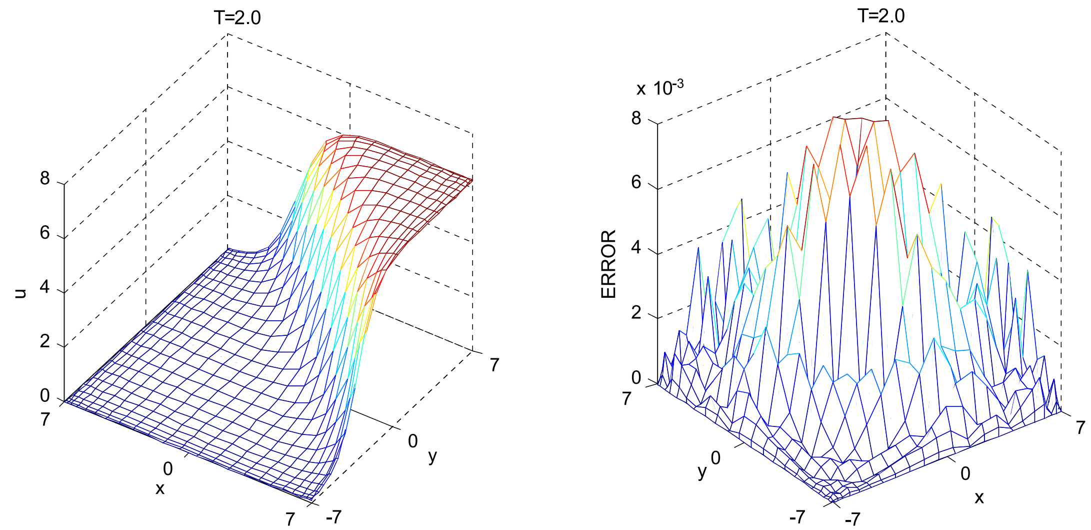

(b) Numerical results for LWSCM at time $t = 2.0$.

Fig. 6. Numerical solutions and error for LWSCM at times $t = 1, 2, 3$ and 4 with $\Delta t = 0.001$ and $N = N' = 24$ for Example 4.

where $f(x, t) = 0$ and subject to the initial conditions

$$\begin{cases} u(x, 0) = 0, & 0 \le x \le 1 \\ u_t(x, 0) = 4\,\mathrm{sech}(x), & 0 \le x \le 1, \end{cases} \tag{4.10}$$

and the Dirichlet boundary condition

$$u(x, t) = h(x, t), \quad x \in \partial\Omega, \ 0 < t \le T. \tag{4.11}$$

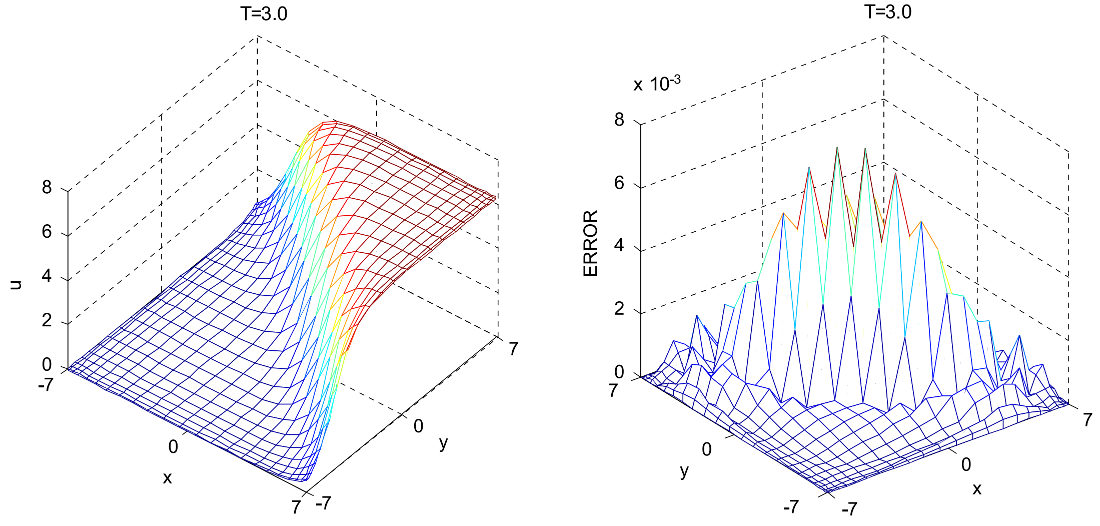

(c) Numerical results for LWSCM at time $t = 3.0$.

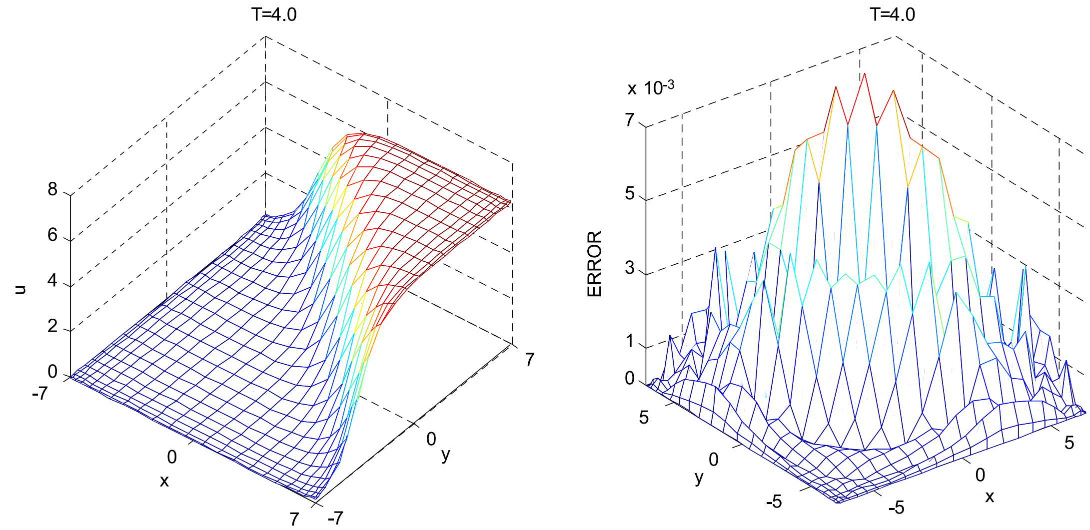

(d) Numerical results for LWSCM at time $t = 4.0$.

Fig. 6. (*continued*)

The exact solution of Eq. (4.9) is

$$u(x, t) = 4 \tan^{-1} (\text{sech}(x)\, t). \tag{4.12}$$

Fig. 4 shows the numerical solutions of Example 3 by using LWSCM with $N = 24$ and $\Delta t = 0.0001$. From Fig. 4, it can be found that the accuracy of LWSCM is higher than one-iterate solution of the variation iterational method. Fig. 5 shows the RSM errors (in log form) as a function of N at $t = 1.0$ with $\Delta t = 0.0001$ and as a function of Δt at $t = 1.0$ with $N = 32$ for Example 3. From Fig. 5, one can conclude that LWSCM still keeps the exponential convergence property.

4.2. 2D case

Example 4. Consider the following two-dimensional nonlinear Sine–Gordon equation [4,14,31]

$$\frac{\partial^2 u}{\partial t^2} + \beta \frac{\partial u}{\partial t} = \frac{\partial^2 u}{\partial x^2} + \frac{\partial^2 u}{\partial y^2} - \sin(u), \quad -7 \le x, y \le 7,\ t > 0, \tag{4.13}$$

with initial conditions

$$u(x,y,0)=4\tan^{-1}(\exp(x+y)), \quad -7\le x,\ y\le 7,\ t>0,$$
$$\frac{\partial u(x,y,0)}{\partial t}=-\frac{4\exp(x+y)}{1+\exp(2x+2y)}, \quad -7\le x,\ y\le 7,\ t>0, \tag{4.14}$$

and boundary conditions

$$\frac{\partial u}{\partial x}=\frac{4\exp(x+y+t)}{\exp(2t)+\exp(2x+2y)}, \quad \text{for } x=-7 \text{ and } x=7,\ -7\le y\le 7,\ t>0, \tag{4.15}$$
$$\frac{\partial u}{\partial y}=\frac{4\exp(x+y+t)}{\exp(2t)+\exp(2x+2y)}, \quad \text{for } y=-7 \text{ and } y=7,\ -7\le x\le 7,\ t>0. \tag{4.16}$$

The theoretical solution of this problem, in which the parameter $\beta = 0$ is given by

$$u(x,y,t)=4\tan^{-1}(\exp(x+y-t)). \tag{4.17}$$

The solution was computed for $(x, y) \in [-7, 7] \times [-7, 7]$ and $t > 0$. The errors in the L_2, L_∞ norms and root-mean-square (RMS) of errors at time $t = 1, 3, 5$ and 7 are given in Table 3. The graphs of numerical solutions for $t = 1, 2, 3$ and 4 are given in Fig. 6. From Table 3, one can find that LWSCM is more accurate than the explicit method [31] and the RBF method [14] while only needs a few number of grid points.

5. Conclusion

In this paper, a new spectral collocation method based on Legendre wavelets basis is proposed and successfully applied for the solution of 1D and 2D Klein/Sine-Gordon equations. The exponential convergence property and error characteristics are shown in these examples. There are three important points to make here. First, LWSCM can provide good spatial resolution and spectral resolution, so can get a high accuracy solution. Second, LWSCM is computer oriented and can establish a connection with fast algorithms. Third, LWSCM can save more memory and computation time benefit from the advantage of Legendre wavelets operational matrices. The numerical results presented here suggest that the Legendre wavelets spectral collocation method is very effective, accurate and easy to implement for the numerical solution of partial differential equations.

Acknowledgment

This work is supported by National Natural Science Foundation of China (Grant No. 41105063).

References

[1] X. Hu, S.Z. Lin, Phase dynamics in a stack of inductively coupled intrinsic Josephson junctions and terahertz electromagnetic radiation, Supercond. Sci. Technol. 23 (2010) 053001.
[2] A.E. Koshelev, Stability of dynamic coherent states in intrinsic Josephson-junction stacks near internal cavity resonance, Phys. Rev. B. 82 (2010) 174512.
[3] V.M. Krasnov, The emission form intrinsic Josephson junctions at zeros magnetic field via breather auto-oscillations, Phys. Rev. B. 83 (2010) 174512.
[4] G. Grella, M. Marinaro, Special solutions of the Sine-Gordon equation in 2 + 1 dimensions, Lett. Nuovo Cimento 23 (1978) (1971–1985) 459–464.
[5] D.B. Duncan, Symplectic finite difference approximations of the nonlinear Klein–Gordon equation, SIAM J. Numer. Anal. 34 (1997) 1742–1760.
[6] I.J. Lee, Numerical solution for nonlinear Klein–Gordon equation by collocation method with respect to spectral method, J. Korean Math. Soc. 32 (1995) 541–551.
[7] G. Ben-Yu, L. Xun, L. Vazquez, A Legendre spectral method for solving the nonlinear Klein–Gordon equation, Comput. Appl. Math. 15 (1996) 19–36.
[8] X. Li, B.Y. Guo, A Legendre spectral method for solving the nonlinear Klein–Gordon equation, J. Comput. Math. 15 (1997) 105–126.
[9] Salah M. El-Sayed, The decomposition method for studying the Klein–Gordon equation, Chaos Solitons Fractals 18 (2003) 1025–1030.
[10] Doğan Kaya, Salah M. El-Sayed, A numerical solution of the Klein–Gordon equation and convergence of the decomposition method, Appl. Math. Comput. 156 (2004) 341–353.
[11] B. Batiha, M.S.M. Noorani, I. Hashim, Numerical solution of Sine-Gordon equation by variational iteration method, Phys. Lett. A 370 (2007) 437–440.
[12] F. Shakeri, M. Dehghan, Numerical solution of the Klein–Gordon equation via He's variational iteration method, Nonlinear Dynam. 51 (2008) 89–97.
[13] M. Dehghan, D. Mirzaei, The boundary integral equation approach for numerical solution of the one-dimensional Sine-Gordon equation, Numer. Methods Partial Differential Equations 24 (2008) 1405–1415.
[14] M. Dehghan, A. Shokri, A numerical method for solution of the two-dimensional Sine-Gordon equation using the radial basis functions, Math. Comput. Simul. 79 (2008) 700–715.
[15] M. Dehghan, A. Shokri, A numerical method for one-dimensional nonlinear Sine-Gordon equation using collocation and radial basis functions, Numer. Methods Partial Differential Equations 24 (2008) 687–698.
[16] M. Dehghan, D. Mirzaei, The dual reciprocity boundary element method (DRBEM) for two-dimensional Sine-Gordon equation, Comput. Methods Appl. Mech. Engrg. 197 (2008) 476–486.
[17] M. Dehghan, A. Shokri, Numerical solution of the nonlinear Klein–Gordon equation using radial basis functions, J. Comput. Appl. Math. 230 (2009) 400–410.
[18] M. Dehghan, A. Ghesmati, Application of the dual reciprocity boundary integral equation technique to solve the nonlinear Klein–Gordon equation, Comput. Phys. Comm. 81 (2010) 1410–1418.
[19] M. Lakestani, M. Dehghan, Collocation and finite difference-collocation methods for the solution of nonlinear Klein–Gordon equation, Comput. Phys. Comm. 181 (2010) 1392–1401.

[20] A. Mohebbi, M. Dehghan, High-order solution of one-dimensional Sine-Gordon equation using compact finite difference and DIRKN methods, Math. Comput. Modelling 51 (2010) 537–549.
[21] D. Mirzaei, M. Dehghan, Meshless local Petrov–Galerkin (MLPG) approximation to the two dimensional Sine-Gordon equation, J. Comput. Appl. Math. 233 (2010) 2737–2754.
[22] B. Pekmen, M. Tezer-Sezgin, Differential quadrature solution of nonlinear Klein–Gordon and Sine-Gordon equations, Comput. Phys. Comm. 183 (2012) 1702–1713.
[23] G. Hariharan, Haar wavelet method for solving the Klein–Gordon and the Sine-Gordon equations, Int. J. Nonlinear Sci. 11 (2011) 180–189.
[24] F. Yin, J. Song, F. Lu, A coupled method of Laplace transform and Legendre wavelets for nonlinear Klein–Gordon equations, Math. Methods Appl. Sci. 37 (2014) 781–791.
[25] S.A. Yousefi, Legendre wavelets method for solving differential equations of Lane–Emden type, Appl. Math. Comput. 181 (2006) 1417–1422.
[26] Fukang Yin, Junqiang Song, Xiaoqun Cao, Fengshun Lu, Couple of the variational iteration method and Legendre wavelets for nonlinear partial differential equations, J. Appl. Math. 2013 (2013) (2013) 11 pages, http://dx.doi.org/10.1155/2013/157956, Article ID 157956.
[27] G. Beylkin, R. Coifman, V. Rokhlin, Fast wavelet transforms and numerical algorithms I, Comm. Pure Appl. Math. 44 (1991) 141–183.
[28] M. Kumar, S. Pandit, Wavelet transform and wavelet based numerical methods: an introduction, Int. J. Nonlinear Sci. 13 (2012) 325–345.
[29] K. Maleknejad, S. Sohrabi, Numerical solution of Fredholm integral equations of the first kind by using Legendre wavelets, Appl. Math. Comput. 186 (2007) 836–843.
[30] F. Mohammadi, M.M. Hosseini, A new Legendre wavelet operational matrix of derivative and its applications in solving the singular ordinary differential equations, J. Franklin Inst. 348 (2011) 1787–1796.
[31] K. Djidjeli, W.G. Price, E.H. Twizell, Numerical solutions of a damped Sine-Gordon equation in two space variables, J. Engrg. Math. 29 (1995) 347–369.
[32] M. Razzaghi, S. Yousefi, Legendre wavelets direct method for variational problems, Math. Comput. Simulation 53 (2000) 185–192.
[33] M. Kumar, S. Pandit, Wavelet transform and wavelet based numerical methods: an introduction, Int. J. Nonlinear Sci. 13 (2012) 325–345.
[34] N. Liu, E.B. Lin, Legendre wavelet method for numerical solutions of partial differential equations, Numer. Methods Partial Differential Equations 26 (2010) 81–94.
[35] A. Karimi Dizicheh, F. Ismail, M. Tavassoli Kajani, Mohammad Maleki, A Legendre wavelet spectral collocation method for solving oscillatory initial value problems, J. Appl. Math. 2013, 5 pages, http://dx.doi.org/10.1155/2013/591636, Article ID 591636.